

Full-length human Surfactant Protein A inhibits Influenza A Virus infection of A549 lung epithelial cells: a recombinant form containing neck and lectin domains promotes infectivity

Ahmed A. Al-Qahtani¹⁺, Valarmathy Murugaiah²⁺, Hani A. Bashir², Ansar A. Pathan², Suhair M. Abozaid¹, Evgeny Makarov², Beatrice Nal², Uday Kishore², Mohammed N. Al-Ahdal^{1*},

¹Department of Infection and Immunity, King Faisal Specialist Hospital and Research Centre, Riyadh, Saudi Arabia

²Biosciences, College of Health and Life Sciences, Brunel University London, Uxbridge UB8 3PH, United Kingdom

*Corresponding Author: Prof. M. N. Al-Ahdal (profahdal@gmail.com)

⁺AAQ and MV are joint first authors.

Running Title: Human SP-A as an immunomodulator against IAV

Keywords: Innate immunity; Influenza A Virus; pulmonary collectins; Surfactant Protein A

Acknowledgement: This work was in part funded by the KACST (14-MED258-20) and approved by the RAC of the KFSHRC, Riyadh (2150031). We are grateful to Maureene Delos Reyes and Hanan Shaarawi for secretarial help and administrative support.

Abstract

Hydrophilic lung surfactant proteins have emerged as key immunomodulators aimed at recognition and clearance of pulmonary pathogens. Surfactant protein A (SP-A) is a surfactant-associated innate immune pattern recognition molecule, which is known to interact with a variety of pathogens, and display anti-microbial effects. SP-A, being carbohydrate pattern recognition molecule, has been suggested to have a wide range of innate immune functions against pathogens. In addition, SP-A can work against respiratory pathogens, including influenza A virus (IAV). Some pandemic pH1N1 strains resist neutralization by SP-A due to differences in the N-glycosylation of viral hemagglutinin (HA). Here, we provide evidence, for the first time, that a recombinant form of human SP-A (rfhSP-A) composed of α -helical neck and carbohydrate recognition domains can actually promote the IAV replication, as observed by an upregulation of M1 expression in lung epithelial cell line, A549, when challenged with pH1N1 and H3N2 IAV subtypes. rfhSP-A (10 μ g/ml) bound neuraminidase (NA) (~60kDa), matrix protein 1 (M1) (~25kDa) and M2 (~17kDa) in a calcium dependent manner, as revealed by far western blotting, and direct binding ELISA. However, human full length native SP-A downregulated mRNA expression levels of M1 in A549 cells challenged with IAV subtypes. Furthermore, qPCR analysis showed that transcriptional levels of TNF- α , IL-12, IL-6, IFN- α and RANTES were enhanced following rfhSP-A treatment by both IAV subtypes at 6 h post-IAV infection of A549 lung epithelial cells. In the case of full length SP-A treatment, mRNA expression levels of TNF- α , and IL-6 were downregulated during the mid-to-late stage of IAV infection of A549 cells. Multiplex cytokine/chemokine array revealed enhanced levels of both IL-6 and TNF- α due to rfhSP-A treatment in the case of both IAV subtypes tested, while no significant effect was seen in the case of IL-12. Enhancement of IAV infection of pH1N1 and H3N2 subtypes by truncated rfhSP-A, concomitant with infection inhibition by full-length SP-A, appears to suggest that a complete SP-A molecule is required for protection against IAV. This is in contrast to a recombinant form of trimeric lectin domains of human SP-D (rfhSP-D) that acts as an entry inhibitor of IAV.

Introduction

The initial response to an infection in a host is the activation of its innate immune system. Understanding how innate immune mechanisms restrict the spread of respiratory infections is crucial to designing therapeutic strategies. Influenza virus has been a major infectious respiratory pathogen, and remains a serious global health concern, resulting in up to half a million respiratory deaths annually (WHO 2018). There are four distinct types of Influenza virus, which have been reported to cause infections in humans; influenza virus A (IAV) represents the most common cause of significant health threat. IAV is responsible for approximately 70% of all influenza related deaths, and has caused highly pathogenic pandemics (WHO 2009). IAV is further classified into different subtypes, depending on the combination of their surface glycoproteins, hemagglutinin (HA) and the neuraminidase (NA) (Bouvier et al., 2008). IAV has been reported to exert a greater selective pressure on the host, with a complex pathogenesis characterised by rapid viral replication, and viral distribution within the lungs, while evoking cellular and humoral immunity (Fukuyama et al., 2011). Although IAV has evolved numerous molecular strategies to avoid and escape the host's immune responses, and to promote continuous survival within the host, a range of immune responses could potentially target any stage of IAV.

The pulmonary surfactant system is composed of abundant proteins and lipids that lower the surface tension of the alveoli, and suggested to play important roles in innate immunity. Its hydrophilic proteins, also called collectins, are soluble collagenous lectins that serve multiple antimicrobial functions against influenza viruses by binding to oligosaccharide structures via conserved carbohydrate recognition domains on the surface of viral particles (van de Wetering et al., 2004). The interaction between IAV and collectins (found within the mammalian serum and pulmonary fluids) leads to anti-viral activity *in vitro* (Reading et al., 1997). Bovine conglutinin and mannose binding protein (MBP) cause inhibition of IAV hemagglutination and neutralisation (Hartley et al., 1992). Other collectins, including surfactant protein A (SP-A) and SP-D, expressed in the lungs, mucosal and epithelial surfaces in the body, are involved in a number of immune functions involving neutralization, agglutination, opsonisation and clearance of pathogens.

SP-A is a collagenous calcium-dependent defense lectins, composed of N terminal domain rich in cysteine, collagen domain, an α -helical coiled-coil neck and C-terminal with carbohydrate recognition domain (CRD) (Kishore et al., 2006; Nayak et al., 2012). The overall structure of

SP-A is made up six of these subunits, which look like a bouquet (Kishore et al., 2006). The trimeric CRD region recognises pathogens by engaging terminal monosaccharide residues or charged patterns on microorganisms, serving as soluble pattern recognition receptors (PRRs). Thus, collagen like region is crucial for the interaction with immune cell-mediated receptors such as calreticulin-CD91 complex to bring about removal of pathogens (Kishore et al., 2006; Gardai et al., 2003).

Direct interaction between SP-A and various viruses results in viral neutralisation and induction of phagocytosis *in vitro*. SP-A can interact with glycoprotein 120 of HIV-1 and suppress infection of CD4⁺ T cells, and enhance HIV-1 transfer via dendritic cells, serving as a dual modulator of HIV-1 infection (Gaiha et al., 2008). SP-A has also been shown to interact with herpes simplex virus type 1 (HSV-1), and mediate phagocytosis of HSV-1 by alveolar macrophages (van Iwaarden et al., 1991). SP-A can bind to the F2 subunit of respiratory syncytial virus (RSV) and neutralise its infectivity (Ghildyal et al., 1999). In the case of IAV, SP-A can bind HA and NA, and inhibit haemagglutination at initial stages. However, pH1N1 pandemic strains are not neutralised by SP-A due to variations in the N-linked glycosylation of HA (Job et al., 2010). We have recently shown a recombinant form of human surfactant protein D, containing homotrimeric neck and CRD region (rfhSP-D), binds HA and reduces M1 expression in A549 cells challenged with pH1N1 and H3N2 strains (Al-Ahdal et al., 2018). In addition, mRNA expression levels of TNF- α , IFN- α , IFN- β , IL-6 and RANTES production were down-regulated following rfhSP-D treatment. Furthermore, rfhSP-D also reduced MDCK cell transduction by H1+N1 pseudotyped lentiviral particles, suggesting a possible therapeutic modality against IAV infection. In this regards, this study was aimed as investigating the possible role of a well-characterised recombinant truncated form of human SP-A (rfhSP-A) made up of trimeric CRDs, using pH1N1 and H3N2 IAV subtypes.

Method and Materials

Virus and antibodies

A/England/2009 (pH1N1) and the A/HK/99 (H3N2) influenza A subtypes were used for most experiments. Vesicular Stomatitis Virus (VSV-G) was used as a control for ELISA. Monoclonal Anti-Influenza Virus NA, A/California/04/2009 (pH1N1) pdm09, Clone 5C12 (produced *in vitro*), NR-42019 and A/Hong Kong/1/1968 (H3N2) (antiserum, Goat), NR-3118 and anti-M1 monoclonal antibody were obtained from BEI Resources, NIAID, NIH, USA. Monoclonal anti-influenza A virus M2 protein was obtained from Abcam.

Cell Culture

Most reagents were purchased from Sigma unless mentioned otherwise. A549 and MDCK cell lines were cultured in complete DMEM containing FBS (10%), L-glutamine (2 mM), penicillin (100 U/ml), streptomycin (100 µg/ml) and sodium pyruvate (1 mM). Cells were cultured at 37°C in a CO₂ incubator until they were 80% cell confluent. Cells were trypsinised (0.5%; 10 min), spun at 1000 rpm for 7', and suspended in complete DMEM. Viable cells were counted via Trypan Blue (0.4%).

Virus purification and infection titre determination

Purification and production of pH1N1 and H3N2 subtypes were carried out as described earlier (Al-Ahdal et al., 2018). MDCK cells were infected with pH1N1 (2×10^4) or H3N2 (3.3×10^4) by incubation at 37°C for 1 h. Post infection, the viral particles were pelleted via 3,000×g centrifugation at 4°C for 10'. Supernatants containing virus particles were then subjected to ultracentrifugation (25,000×g, 4°C, 1 h 30'), followed by re-suspending virus in 100µl of PBS. 15µl of virus stock was assessed via reduced SDS-PAGE and ELISA. Tissue culture infectious dose (TCID₅₀) assay was performed to determine the infectious titre of the purified pH1N1 and H3N2 viral stocks, and to assess its cytopathic effects (CPE) using MDCK cells, as reported recently (Al-Ahdal et al., 2018). CPE effects of infected and non-infected cells were microscopically examined at each viral dilution.

Production of rfhSP-A

DNA sequences coding for trimeric neck and CRD region were cloned under T7 promoter and expressed in *Escherichia coli* BL21 (λDE3) pLysS using construct pUK-A1 (Karbani et al., 2014). *E. coli* cells were grown in LB medium, containing 100 µg/ml ampicillin and 34 µg/ml of chloramphenicol at 37°C until an OD₆₀₀ reached of 0.6. Following induction with 0.5mM isopropyl β-D-thiogalactoside (IPTG), the bacterial culture was left to grow further for another 3 h on a shaker at 37°C. The bacterial cell pellet was then centrifuged (4500 rpm, 4°C, 10') and re-suspended in lysis buffer (0.05 M Tris-HCL pH 7.5, 0.2M NaCl, 0.005 M EDTA, 0.1% Triton X-100, 0.1 mM phenylmethane sulfonyl fluoride (PMSF), 50 µg lysozyme) for 1 hour at 4°C. The lysate was sonicated using a Soniprep 150 (MSE, London, UK) at 60 Hz for 30 seconds with an interval of 2 min (12 cycles), followed by centrifugation at 12000 rpm for 15 minutes. The inclusion bodies were denatured fully in 50 ml of 0.5 M Tris-HCl, 0.1M NaCl, pH7.5 and 8 M urea for 1 h at 4°C. The soluble fraction was dialysed against the same buffer containing 4 M, 2 M, 1 M and no urea for 2 h at each urea concentration. The refolded material

was then extensively dialysed against affinity buffer that contained 10 mM CaCl₂ instead of 5 mM EDTA for 2 h. The supernatant was loaded on a 5ml of mannose-sepharose column, and bound rfhSP-A was eluted with buffer with 10mM EDTA. Purified rfhSP-A was run on SDS-PAGE to assess its purity. LPS was removed using Endotoxin Removal Resin. LPS level was determined using QCL-1000 Limulus ameobocyte lysate system (Lonza) and found to be ~5 pg/μg of rfhSP-A.

Extraction of full length native SP-A from human bronchoalveolar lavage fluid

Human full-length native SP-A (FLSP-A) was purified as published earlier by Strong et al. (Strong et al., 1998). Bronchoalveolar lavage fluid (BAL) collected from pulmonary alveolar proteinosis patients was made up with buffer I containing 20 mM Tris-HCl and 10mM EDTA, pH 7.4, followed by centrifugation at 10,000 × g. The centrifuged cell pellet was extracted using buffer I with 6 M urea. The solubilised FLSP-A was centrifuged again at 10,000 × g and the soluble fraction was dialysed against 4, 2, and 1 M urea in buffer II (20 mM Tris-HCl, 100 mM NaCl, and 5 mM EDTA, pH 7.4). The supernatant was again dialysed against buffer II containing 15mM CaCl₂, and loaded onto maltose agarose column, followed by elution with 10 mM EDTA.

SDS-PAGE Electrophoresis

SDS-PAGE 12% (w/v) was performed to analyse and detect the purity of purified rfhSP-A and FLSP-A. Purified proteins were diluted in 1:1 (v/v) ratio in 2× Laemmli sample buffer (10ml) (Bio-Rad, Hertfordshire, catalogue no.161-0737) containing 1M Tris-HCL (PH 6.8, 1ml), 10% SDS (4ml), 100% Glycerol (2ml), 1% Bromophenol blue, β-mercaptoethanol (2.5ml) and distilled water (d.H₂O) (Bio-Rad, Hertfordshire). The protein was then denatured for 10 minutes at 95°C before loading onto 12% (w/v) SDS-PAGE. Standard pre-stained protein marker (Fisher Scientific) was also loaded to assess the size of the purified rfhSP-A. The SDS-PAGE gel was stained overnight using staining solution (1g of Brilliant Blue, 50% (v/v) methanol, 10% acetic acid and 40ml of D.H₂O). The stained gel was then de-stained using the de-staining solution 40% (v/v) methanol, 10% (v/v) acetic acid until the protein bands were visible.

Direct Binding ELISA

The interaction between rfhSP-A and IAV subtypes was measured via direct ELISA. A varied concentrations of FLSP-A, rfhSP-A, rfhSP-D and VSV-G (as a negative control protein) (10,

5, 2.5, and 1.25 µg/well) were coated on microtitre wells of a Maxisorp 96 well plate (Sigma-Aldrich) in carbonate bicarbonate buffer, pH 9.6 and incubated at 4°C overnight. After washing with PBS three times, the unoccupied sites on the wells were blocked with 2% w/v BSA for 2 h at 37°C, and then followed by washing with PBST (PBS + 0.05% Tween 20). pH1N1/H3N2 virus (20 µl of 1.36×10^6 pfu/ml) was diluted 10 times using PBS, and 10 µl of it incubated in the wells for 2 h at RT. After washing, monoclonal anti-H1 and polyclonal anti-H3 (both from BEI-Resources) in PBS (1:5000) were added to the appropriate wells and incubated at 37°C for 1 h, followed by 1 h incubation with rabbit anti-mouse and protein A conjugated to HRP (1:5000) (both from Fisher Scientific). TMB was used as a substrate and the plate was read at OD₄₅₀.

Far Western Blotting

Purified pH1N1/H3N2 (1.36×10^6 pfu/ml) was run on SDS-PAGE and then separated proteins were transferred to a PVDF membrane using transfer buffer (0.25 M Tris, 0.19 M glycine and 20% methanol). After blocking the membrane with 5% w/v milk powder in PBS at 4°C and washing, the membrane was probed with monoclonal anti-NA, M1 or M2 (1:1,000 dilutions) antibodies for 1h at RT. For far-western blotting, the membrane was incubated with 5µg/ml of rfhSP-A in 5mM CaCl₂ buffer overnight at 4°C. Binding was probed with rabbit anti-human SP-A in PBS (1:1000) for 1h at RT. Rabbit anti-mouse and Protein A conjugated to HRP (1:5000) (Fisher Scientific) were used as respective conjugates/secondary probes for polyclonal and monoclonal antibodies. The colour was developed using DAB as a substrate and H₂O₂.

Cell-Binding assay

A549 cells (10,000 cells per well) were seeded in complete DMEM and incubated at 37°C until 80% confluence was reached. After washing with different concentration of purified rfhSP-A (1.25 to 10 µg/ml) were pre-treated with pH1N1/H3N2 virus (1.36×10^6 pfu/ml). 10µl of diluted virus stock was added to the appropriate wells, and incubated for 2 h at RT. After fixing the wells with 4% v/v paraformaldehyde (Fisher Scientific) for 10' at RT, blocking step was carried out using 2% w/v BSA as described above. Anti-H1 and H3 antibodies and secondary probes were used, as described earlier, using TMB as a substrate.

Quantitative RT-PCR

rfhSP-A and FLSP-A (10 µg/ml) was added to A549 cells (0.5×10^6) in DMEM + 5mM CaCl₂ with MOI 1 of H1N1/H3N2 virus and pelleted at different time points. Total RNA was extracted from the above-mentioned cells using GenElute Mammalian Total RNA Purification Kit (Sigma-Aldrich, UK). Total RNA was treated with DNase I (Sigma-Aldrich, UK) prior to assessing concentration and purity of total RNA via reading at OD₂₆₀ and OD₂₆₀:OD₂₈₀ (NanoDrop 2000/2000c; Thermo Fisher Scientific). 2 µg of RNA was converted into cDNA using cDNA Kit (Applied Biosystems). qRT-PCR was performed using the 7900HT Fast Real-Time PCR System (Applied Biosciences). Each reaction was carried out in triplicates and included 5µl Power SYBR Green MasterMix, 75 nM of FP and RP, and 500 ng cDNA. The amplification cycle involved 50°C and 95°C for 2' and 10', followed by 40 cycles of amplification. Human 18S rRNA was used to normalise gene expression and as an endogenous control.

Multiplex cytokine array analysis

In order to measure the secreted cytokines and chemokines following rfhSP-A treatment, IAV treated A549 cells were incubated in the presence or absence of rfhSP-A (10 µg/ml) for 24 h. Subsequently, supernatants were collected for measuring IL-6, TNF- α , IL-8, IL12 (p40) and MCP-1. The expression levels of various analytes were measured using EMD Millipore multiplex kit. As per manufacture's instruction, 25µl assay buffer was added to microtiter wells, plus 25µl standard, control or supernatant of A549 cells. Magnetic beads (25 µl) linked-analytes were added to each well and incubated at 4°C for 18 h. After assay buffer washing, detection antibodies (25µl) were incubated with beads at RT for 1 h. 25µl of Streptavidin-Phycoerythrin was then added to each well and incubated for 30 mins at RT. After another round of washing, 150 µl of sheath fluid was added to each well and the plate was read using the Luminex Magpix instrument.

Statistical Analysis

GraphPad Prism 6.0 software was used to generate all the graphs. Two-way ANOVA test was used to perform the statistical analysis, and the significance values were considered between rfhSP-A treated and untreated conditions based on * $p < 0.1$, ** $p < 0.05$, *** $p < 0.01$, and **** $p < 0.001$. Error bars show the SD or SEM (figure legends).

Results

Interaction of affinity purified rfhSP-A with pH1N1/H3N3 viral particles

The affinity purified and LPS-free rfhSP-A was evident as a single band at ~18 kDa on 15% SDS-PAGE (v/v) under reducing condition (Figure 1). The direct binding interaction of FLSP-A, rfhSP-A, and rfhSP-D with pH1N1/H3N2 viral particles were determined using ELISA. As shown in figure 2, FLSP-A, rfhSP-A and rfhSP-D bound IAV subtypes in a dose and calcium-dependent manner. No significant binding was observed with VSV-G pseudotyped lentivirus (negative control RNA virus). Cell binding assay was also performed to assess the interaction of rfhSP-A with A549 lung epithelial cells challenged with pH1N1 and H3N2 (Figure 3). Maximum cell binding was seen with 10 µg/ml in both IAV subtypes, while a clear dose dependent binding was seen with H3N2, compared to pH1N1.

rfhSP-A interaction with NA, M1, and M2 proteins of pH1N1 and H3N2

Binding of rfhSP-A to NA (~60 kDa), M1 (~25kDa) and M2 (~17 kDa) of purified pH1N1 and H3N2 was established using far western blotting (Figure 4A). The ability of rfhSP-A to bind immobilised purified recombinant NA was assessed using ELISA. As shown in figure 4C, rfhSP-A interacted with NA dose- and calcium-dependently; VSV-G-pseudotyped particles did not show significant binding. Polymerization of M1 is suggested to provide a crucial mechanism for the elongation of filamentous IAV virions. In addition, rfhSP-A was also found to bind matrix protein 2 (M2) migrating at ~17kDa, as evident from western blotting (Figure 4A). Binding of rfhSP-A to M2 protein may suggest enhancement of viral replication by stabilising the viral budding site, enabling M2 polymerization leading to formation of filamentous viral particles.

rfhSP-A promotes, while FLSP-A inhibits, infection of A549 cells by IAV

Infection assay was performed to determine the ability of IAV to infect A549 cells in the presence or absence of FLSP-A and rfhSP-A (10 µg/ml). rfhSP-A treatment up-regulated M1 expression in infected A549 cells when compared to untreated cells challenged only with virus (Figure 5). In the case of both IAV subtypes, rfhSP-A treatment upregulated M1 expression at 2 and 6 h. The up-regulation of M1 expression was more pronounced for H3N2 than pH1N1, where 7log₁₀ fold up-regulation was noted at 6 h (Figure 5A). M1 is known to bind cytoplasmic ends of HA and NA of IAV, allowing M1 association with lipid raft membrane, and inducing change in its conformation and polymerization at the site of virus budding (Gómez-Puertas et

al., 2000). However, FLSP-A caused downregulation of M1 expression at 2h and 6h in the case of both IAV subtypes. The suppression of M1 following FLSP-A treatment was more evident in the case of pH1N1 when compared to H3N2, where $-5 \log_{10}$ fold reduction was seen at 6h (Figure 5B). This data is consistent with another study using rfhSP-D, where $-8 \log_{10}$ fold downregulation of M1 expression was seen with pH1N1 at 2h (Al-Ahdal et al., 2018).

qRT-PCR analysis of modulation of immune responses by rfhSP-A on A549 challenged with IAV subtypes

The mRNA levels of pro-inflammatory cytokines and chemokines were determined via qPCR. The relative mRNA levels of TNF- α , IL-12, IFN- α , and RANTES were upregulated by both IAV strains, following rfhSP-A treatment at 6h time point. However, IL-6 was $2 \log_{10}$ fold upregulated by pH1N1 at 6h by rfhSP-A treatment (Figure 6A), but no significance change was found with H3N2 strain at 6h. Furthermore, enhancement of IFN- α was also evident with rfhSP-A treatment at both 2h, which gradually declined by $2 \log_{10}$ fold at 6h (Figure 7A). Upregulation of type I interferon may suggest that rfhSP-A can enhance viral replication, and thus, increase the levels of interferon type I response to alert other immune cells to mobilise mechanisms towards viral clearance. In the case of FLSP-A treatment, pro-inflammatory cytokines such as TNF- α and IL-6 were downregulated at 6h treatment in both pH1N1 and H3N2 (Figure 6C & D). Enhanced level of IL-6 has been reported in patients infected with pH1N1 (Paquette et al., 2012). IL-12 ($-2 \log_{10}$ fold) and RANTES ($-6.5 \log_{10}$ fold) were downregulated by FLSP-A treatment in pH1N1 subtype (Figure 6C), while upregulation was seen with H3N2 (Figure 6D), suggesting the possible enhancement of Th1 immune response. In the case of type I interferons, FLSP-A has induced upregulation of IFN- α at 6h in both IAV strains.

Multiplex analysis of cytokine/chemokine array following rfhSP-A treatment

Secretion of cytokines and chemokines, 24h post rfhSP-A treatment, was assessed using a multiplex cytokine/chemokine array. rfhSP-A triggered enhancement of TNF- α , IL-6 and IL-8 in both IAV subtypes (Figure 8). However, no significance effect was seen with MCP-1 for both IAV subtypes. Increased IL-6 level has been linked with the severity of IAV infection based on a study involving pH1N1-infected mice (Paquette et al., 2012). Expression of TNF- α in lung epithelial cells is suggested to be the key targets of IAV, and appeared to be important to control IAV in the host respiratory tract. TNF- α is involved in recruiting monocytes, T and B lymphocytes to the site of infection, suggesting that its role in clearing the viral particles in

the respiratory tract prior to the induction of secondary immune response. Therefore, up-regulation of TNF- α and IL-6 by rfhSP-A can serve as a potential biomarker during IAV infection, similar to other diseases (Damas et al., 1992; Theoharides et al., 2002).

Discussion

Influenza A virus (IAV) is a contagious respiratory virus, causing substantial morbidity and mortality. Anders et al first reported collectins as beta inhibitors derived from bovine and mouse. The calcium dependent mannose binding lectin (MBL) was shown to bind glycans found on the globular region of HA, thus, inhibiting HA from binding to sialic acid-decorated cell-surface receptors (Anders et al., 1990). Collectins can orchestrate a number of anti-IAV mechanisms such as inhibition of HA and NA (Hartshorn et al., 1994; 2008; Al-Ahdal et al., 2018), virus neutralisation, virus aggregation, IAV uptake by neutrophils, and viral opsonisation. SP-A is a calcium-dependent hydrophilic C-type collectin, involved in pulmonary surfactant homeostasis (Weaver et al., 1991), and reported to be a potent innate immune molecule in the lungs. SP-A can bind various self and non-self-ligands in a calcium-dependent manner, mostly via CRD region on the target surface. Thus, recruitment and activation of immune cells occurs via collagen domain for the clearance of microorganisms (Kishore et al., 2006). SP-A can bind a diverse group of pathogens, acting as opsonins leading to direct and indirect biological consequences (Crouch et al., 2000, Lawson et al., 2000, Crouch et al., 2001). Specific interaction of SP-A with a number of respiratory viruses has been reported, which requires interaction between viral glycoproteins and complex oligosaccharides found on SP-A. Recently, we described a protective effect of rfhSP-D that was able to inhibit entry of IAV into A549 cells challenged with pH1N1 and H3N2 subtypes (Al-Ahdal et al., 2018). Therefore, this study was aimed at examining the direct interaction of a truncated recombinant fragment of human SP-A (rfhSP-A) with IAV, and subsequent immunological consequences.

In this study, protein-protein interaction between rfhSP-A and IAV subtypes (pH1N1 and H3N2). Plasmid pUK-A1, containing cDNA sequences for neck and CRD region of human SP-A (Karbani et al., 2014) was transformed in *Escherichia coli* BL21 (λ DE3) pLysS strain under T7 bacteriophage promoter. rfhSP-A, recovered from inclusion bodies via denaturation-renaturation cycles, was affinity purified on a mannose-agarose column, which appeared as a ~18kDa band on a 15% SDS-PAGE gel electrophoresis (Figure 1). rfhSP-A eluted as a trimer on a gel filtration column and was recognised by rabbit polyclonal and mouse monoclonal

antibodies raised against full length SP-A purified from lung lavage of an alveolar proteinosis patient (data not shown). Affinity purified rfhSP-A made free from endotoxin, was then examined for its respective interaction with IAV subtypes (pH1N1 and H3N2) via direct ELISA (Figure 2). The ability of FLSP-A, rfhSP-A and rfhSP-D to bind IAV subtypes is consistent with an earlier study using a recombinant form of truncated human SP-D (rfhSP-D) composed of trimeric neck and CRD region (Al-Ahdal et al., 2018).

The 10 µg/ml of rfhSP-A bound best to both pH1N1 and H3N2 (Figure 2). The ability of rfhSP-A to bind IAV bound A549 cells was measured via cell binding assay (Figure 3). To understand whether interaction between rfhSP-A and IAV subtypes led to specific interaction with IAV glycoproteins, far western blotting analysis was carried out (Figure 4A). rfhSP-A (10 µg/ml) bound to NA (~60 kDa), M1 (~25kDa) and M2 (~17kDa) of purified pH1N1 and H3N2 in a calcium-dependent manner. Furthermore, in order to validate the binding interaction rfhSP-A and NA, an ELISA was carried out using purified recombinant NA protein. As evident in figure 4B, rfhSP-A bound purified NA protein dose-dependently. Previous studies have also suggested that full length SP-A can bind to NA, and inhibit the release of viral particles from infected cells (Teclé et al., 2007). Thus, N-linked oligosaccharides found on NA are likely to be recognised by the CRD region of SP-A and SP-D (Teclé et al., 2007).

The ability of rfhSP-A to modulate viral replication and enhance host response immune response by IAV challenged A549 cells following rhSP-A treatment was also examined. IAV-bound rfhSP-A was found to induce enhanced viral replication, based on the expression levels of M1 gene. M1 is an abundant matrix protein of IAV, which plays dual roles in virion assembly and infection (Rossman et al., 2011). Up-regulation of M1 expression was brought about by rfhSP-A treatment in IAV challenged A549 cells, compared to cells without rfhSP-A treatment but challenged with pH1N1 or H3N2 only (Figure 5). M1 upregulation, following rfhSP-A treatment was effective in H3N2 infected cells compared to pH1N1, where 7log₁₀ fold upregulation was seen at 6 h (Figure 5). However, A549 cells, pre-treated with FLSP-A, caused downregulation of M1 expression when compared to cells only challenged with IAV subtypes (Figure 5B). M1 downregulation by FLSP-A was found to be more effective in pH1N1 subtype, when compared to H3N2, where -5 log₁₀ fold downregulation was evident at 6h treatment (Figure 5B). M1 can bind cytoplasmic ends of HA and NA, polymerize and form the interior structure of emerging viral particles (Rossman et al., 2011). Additionally, as evident in far western blotting, rfhSP-A was also able to bind Matrix protein 2 (M2) of IAV at ~17 kDa (Figure 4). HA bound M1 also suggested to serve as docking site for the viral RNPs recruitment

and may mediate M2 recruitment to the site of viral budding (Rossman et al., 2011). M2 can stabilise the budding site, enabling polymerization of the matrix protein, leading to formation of viral particles. Furthermore, M2 has also been reported to change so as to facilitate release of the progeny viral particles. Binding of rfhSP-A to NA/M1/M2, and upregulation of M1 expression could suggest the likely role of rfhSP-A as a facilitator of IAV replication of subtypes tested in this study.

mRNA expression of pro-inflammatory cytokines and chemokines following rfhSP-A treatment were determined by qPCR. Our qPCR data showed an upregulation of TNF- α , IL-12 and RANTES in the case of both IAV subtypes at 6h time point. However, an increased expression levels of IL-6 (2log₁₀ fold) (Figure 6A) was seen only with pH1N1 at 6h, while H3N2 did not show any significant effect (Figure 6B). In contrast, downregulation of TNF- α (-4.5 log₁₀ fold) and IL-6 (-5 log₁₀ fold) was seen at 6h following FLSP-A treatment (Figure 6C & D). In the case of pH1N1, FLSP-A also caused downregulation of IL-12 and RANTES mRNA expression (Figure 6C), while increased expression levels was observed with H3N2 IAV subtype (Figure 6D). Enhanced levels of TNF- α and IL-6 have been reported during IAV infection, and it is also associated with severe lung pathology and worse outcome in IAV infected patients (La Gruta et al., 2007). However, these cytokines can also be protective during seasonal influenza infection. Studies also report increased level of IL-6 in the lungs and serum of patients infected with influenza virus, including the outbreak 2009 pH1N1 pandemic subtype (Kaiser et al., 2001, Hagau et al., 2010), which is being examined in this study. Therefore, increased levels of IL-6 following rfhSP-A treatment may be associated with facilitation of IAV infection, and acute lung injury.

Increased serum levels of TNF- α has been reported in most influenza infected patients, particularly pH1N1 subtype (Hagau et al., 2010, Zúñiga et al., 2011, Bermejo-Martin et al., 2010, Morales-García et al., 2012). In this study, when pH1N1 and H3N2 were treated with rfhSP-A, TNF- α expression levels were enhanced at 6 h (Figure 6), suggesting the ability of rhSP-A to increase viral infection, or virus-mediated respiratory diseases. Overexpression of TNF- α and IL-6 has been suggested as a hallmark of viral infection (Mogensen et al., 2001). Elevated levels of these cytokines haven been observed in patients with both acute (Kaiser et al., 2001) and severe (Heltzer et al., 2009) seasonal IAV infection. Up-regulation of cytokines production upon H1N1 infection has been reported as an important crucial player in the pathogenesis of IAV infection. Thus, invasion of H1N1 strain into the lungs has been reported

to trigger production of pro-inflammatory cytokine profile, resulting in the development of pneumonia.

rfhSP-A treatment caused increased levels of IL-12 by both pH1N1 and H3N2 in a time dependent manner (Figure 6), suggesting the likely enhancement of viral replication and Th1 immune response. RANTES was down-regulated in the presence of rfhSP-A at 2h, which recovered by 2.5log₁₀ fold later at 6 h time point in pH1N1 treated cells. However, for H3N2, only 1log₁₀ fold upregulation was seen following rfhSP-A treatment in a time-dependent manner (Figure 6B). Lower expression levels of IFN- α was observed in the untreated sample, which was 3log₁₀ fold up-regulated in the presence of rfhSP-A at 2h (Figure 7), suggesting that rfhSP-A can enhance the rate of viral replication, and thus, thereby enhance the levels of IFN produced by the innate immune cells in order to clear viral particles from infected host.

In conclusion, a truncated recombinant form of human SP-A, rfhSP-A, can promote pH1N1 and H3N2 subtypes of IAV instead of inhibition of infection. We have previously shown that its SP-D counterpart acts as an entry inhibitor (Al-Ahdal et al, 2018), suggesting that rfhSP-A may not have a therapeutic value. The effects of FLSP-A on IAV challenged A549 cells is similar to the effect seen by rfhSP-D, where downregulation of M1 and pro-inflammatory cytokines were seen with FLSP-A treatment. The observed restriction of M1 replication following FLSP-A treatment is likely to be due to the presence of collagen region, which could shift the way SP-A acts on IAV infectivity involving its putative receptor on the cell surface (Gardai et al, 2003). This study highlights a fundamental difference in the structure-function relationships between SP-A and SP-D. The literature is full of evidences where a recombinant truncated form of human SP-D (rfhSP-D) containing trimeric neck and CRD regions behave like full-length SP-D *in vitro*, *in vivo* and *ex vivo*, including offering a protective effect against IAV. In the case of SP-A and IAV interaction, it appears that only FLSP-A is capable of interfering with IAV entry into the target cells, highlighting the importance of the collagen domain and an intact SP-A molecule. It is also apparent that entry inhibition is coupled with an anti-inflammatory response, as evident from downregulation of TNF- α and IL-6. However, both FLSP-A as well as rfhSP-A upregulate type I interferon (IFN- α) response, raising the notion that FLSP-A creates an anti-inflammatory milieu during IAV infection. How rfhSP-A on its own enhances IAV infection remains an intriguing question. We are currently examining the mechanism of enhanced infectivity that may involve topological alterations in M1 and M2 proteins leading to an exaggerated budding.

References

Al-Ahdal MN, Murugaiah V, Varghese PM, Abozaid SM, Saba I, Al-Qahtani AA, Pathan AA, Kouser L, Nal B, Kishore U. Entry Inhibition and Modulation of Pro-Inflammatory Immune Response Against Influenza A Virus by a Recombinant Truncated Surfactant Protein D. *Front Immunol.* 2018 Jul 30;9:1586. doi: 10.3389/fimmu.2018.01586. eCollection 2018.

Anders EM, Hartley CA, Jackson DC. Bovine and mouse serum beta inhibitors of influenza A viruses are mannose-binding lectins. *Proc Natl Acad Sci U S A.* 1990 Jun;87(12):4485-9.

Bermejo-Martin JF, Martin-Loeches I, Rello J, Antón A, Almansa R, Xu L, Lopez-Campos G, Pumarola T, Ran L, Ramirez P, Banner D, Ng DC, Socias L, Loza A, Andaluz D, Maravi E, Gómez-Sánchez MJ, Gordón M, Gallegos MC, Fernandez V, Aldunate S, León C, Merino P,

Blanco J, Martin-Sanchez F, Rico L, Varillas D, Iglesias V, Marcos MÁ, Gandía F, Bobillo F, Nogueira B, Rojo S, Resino S, Castro C, Ortiz de Lejarazu R, Kelvin D. Host adaptive immunity deficiency in severe pandemic influenza. *Crit Care.* 2010;14(5):R167. doi: 10.1186/cc9259. Epub 2010 Sep 14.

Bouvier NM, Palese P. The biology of influenza viruses. *Vaccine.* 2008 Sep 12;26 Suppl 4:D49-53.

Crouch E, Wright JR. Surfactant proteins A and D and pulmonary host defense. *Annu Rev Physiol.* 2001;63:521-54.

Crouch EC. Surfactant protein-D and pulmonary host defense. *Respir Res.* 2000;1(2):93-108. Epub 2000 Aug 25

Damas P, Ledoux D, Nys M, Vrindts Y, De Groote D, Franchimont P, Lamy M. Cytokine serum level during severe sepsis in human IL-6 as a marker of severity. *Ann Surg.* 1992 Apr;215(4):356-62.

Fukuyama S, Kawaoka Y. The pathogenesis of influenza virus infections: the contributions of virus and host factors. *Curr Opin Immunol.* 2011 Aug;23(4):481-6. doi: 10.1016/j.coi.2011.07.016. Epub 2011 Aug 11.

Gaiha GD, Dong T, Palaniyar N, Mitchell DA, Reid KB, Clark HW. Surfactant protein A binds to HIV and inhibits direct infection of CD4+ cells, but enhances dendritic cell-mediated viral transfer. *J Immunol.* 2008 Jul 1;181(1):601-9.

Gardai SJ, Xiao YQ, Dickinson M, Nick JA, Voelker DR, Greene KE, Henson PM. By binding SIRPalpha or calreticulin/CD91, lung collectins act as dual function surveillance molecules to suppress or enhance inflammation. *Cell.* 2003 Oct 3;115(1):13-23.

Ghildyal R, Hartley C, Varrasso A, Meanger J, Voelker DR, Anders EM, Mills J. Surfactant protein A binds to the fusion glycoprotein of respiratory syncytial virus and neutralizes virion infectivity. *J Infect Dis.* 1999 Dec;180(6):2009-13

Gómez-Puertas P, Albo C, Pérez-Pastrana E, Vivo A, Portela A. Influenza virus matrix protein is the major driving force in virus budding. *J Virol.* 2000 Dec;74(24):11538-47.

Hagau N, Slavcovici A, Gonganau DN, Oltean S, Dirzu DS, Brezozski ES, Maxim M, Ciuce C, Mlesnite M, Gavrus RL, Laslo C, Hagau R, Petrescu M, Studnicska DM. Clinical aspects and cytokine response in severe H1N1 influenza A virus infection. *Crit Care.* 2010;14(6):R203. doi: 10.1186/cc9324. Epub 2010 Nov 9.

Hagau N, Slavcovici A, Gonganau DN, Oltean S, Dirzu DS, Brezozski ES, Maxim M, Ciuce C, Mlesnite M, Gavrus RL, Laslo C, Hagau R, Petrescu M, Studnicska DM. Clinical aspects and cytokine

response in severe H1N1 influenza A virus infection. *Crit Care*. 2010;14(6):R203. doi: 10.1186/cc9324. Epub 2010 Nov 9.

Hartley CA, Jackson DC, Anders EM. Two distinct serum mannose-binding lectins function as beta inhibitors of influenza virus: identification of bovine serum beta inhibitor as conglutinin. *J Virol*. 1992 Jul;66(7):4358-63.

Hartshorn KL, Crouch EC, White MR, Eggleton P, Tauber AI, Chang D, et al. Evidence for a protective role of pulmonary surfactant protein D (SPD) against influenza A viruses. *J Clin Invest* (1994) 94:311–9. doi:10.1172/JCI117323

Hartshorn KL, Webby R, White MR, Teclé T, Pan C, Boucher S, et al. Role of viral hemagglutinin glycosylation in anti-influenza activities of recombinant surfactant protein D. *Respir Res* (2008) 9:65–9921–9–65. doi:10.1186/1465-9921-9-65 5.

Heltzer ML, Coffin SE, Maurer K, Bagashev A, Zhang Z, Orange JS, Sullivan KE. Immune dysregulation in severe influenza. *J Leukoc Biol*. 2009 Jun;85(6):1036-43. doi: 10.1189/jlb.1108710.

Job ER, Deng YM, Tate MD, Bottazzi B, Crouch EC, Dean MM, Mantovani A, Brooks AG, Reading PC. Pandemic H1N1 influenza A viruses are resistant to the antiviral activities of innate immune proteins of the collectin and pentraxin superfamilies. *J Immunol*. 2010 Oct 1;185(7):4284-91. doi: 10.4049/jimmunol.1001613. Epub 2010 Sep 3.

Kaiser L, Fritz RS, Straus SE, Gubareva L, Hayden FG. Symptom pathogenesis during acute influenza: interleukin-6 and other cytokine responses. *J Med Virol*. 2001 Jul;64(3):262-8.

Kaiser L, Fritz RS, Straus SE, Gubareva L, Hayden FG. Symptom pathogenesis during acute influenza: interleukin-6 and other cytokine responses. *J Med Virol*. 2001 Jul;64(3):262-8.

Karbani N, Dodagatta-Marri E, Qaseem AS, Madhukaran P, Waters P, Tsolaki AG, Madan T, Kishore U. Purification of native surfactant protein SP-A from pooled amniotic fluid and bronchoalveolar lavage. *Methods Mol Biol*. 2014;1100:257-72. doi: 10.1007/978-1-62703-724-2_21.

Kishore U, Greenhough TJ, Waters P, Shrive AK, Ghai R, Kamran MF, Bernal AL, Reid KB, Madan T, Chakraborty T. Surfactant proteins SP-A and SP-D: structure, function and receptors. *Mol Immunol*. 2006 Mar;43(9):1293-315. Epub 2005 Oct 5

La Gruta NL, Kedzierska K, Stambas J, Doherty PC. A question of self-preservation: immunopathology in influenza virus infection. *Immunol Cell Biol*. 2007 Feb-Mar;85(2):85-92. Epub 2007 Jan 9.

Lawson PR, Reid KB. The roles of surfactant proteins A and D in innate immunity. *Immunol Rev*. 2000 Feb;173:66-78.

Madan T, Reid KB, Clark H, Singh M, Nayak A, Sarma PU, Hawgood S, Kishore U. Susceptibility of mice genetically deficient in SP-A or SP-D gene to invasive pulmonary aspergillosis. *Mol Immunol*. 2010 Jun;47(10):1923-30. doi: 10.1016/j.molimm.2010.02.027.

Mogensen TH, Paludan SR. Molecular pathways in virus-induced cytokine production. *Microbiol Mol Biol Rev*. 2001 Mar;65(1):131-50.

Morales-García G1, Falfán-Valencia R, García-Ramírez RA, Camarena Á, Ramirez-Venegas A, Castillejos-López M, Pérez-Rodríguez M, González-Bonilla C, Grajales-Muñiz C, Borja-Aburto V, Mejía-Aranguré JM. Pandemic influenza A/H1N1 virus infection and TNF, LTA, IL-1 β , IL-6, IL-8, and CCL polymorphisms in Mexican population: a case-control study. *BMC Infect Dis*. 2012 Nov 13;12:299. doi: 10.1186/1471-2334-12-299.

- Nayak A, Dodagatta-Marri E, Tsolaki AG, Kishore U. An Insight into the Diverse Roles of Surfactant Proteins, SP-A and SP-D in Innate and Adaptive Immunity. *Front Immunol.* 2012 Jun 7;3:131. doi: 10.3389/fimmu.2012.00131. eCollection 2012.
- Paquette SG, Banner D, Zhao Z, Fang Y, Huang SS, León AJ, Ng DC, Almansa R, Martin-Loeches I, Ramirez P, Socias L, Loza A, Blanco J, Sansonetti P, Rello J, Andaluz D, Shum B, Rubino S, de Lejarazu RO, Tran D, Delogu G, Fadda G, Krajden S, Rubin BB, Bermejo-Martin JF, Kelvin AA, Kelvin DJ. Interleukin-6 is a potential biomarker for severe pandemic H1N1 influenza A infection. *PLoS One.* 2012;7(6):e38214. doi: 10.1371/journal.pone.0038214. Epub 2012 Jun 5.
- Reading PC, Morey LS, Crouch EC, Anders EM. Collectin-mediated antiviral host defense of the lung: evidence from influenza virus infection of mice. *J Virol.* 1997 Nov;71(11):8204-12.
- Rossman JS, Lamb RA. Influenza virus assembly and budding. *Virology.* 2011 Mar 15;411(2):229-36. doi: 10.1016/j.virol.2010.12.003. Epub 2011 Jan 14.
- Strong P, Kishore U, Morgan C, Lopez Bernal A, Singh M, Reid KB. A novel method of purifying lung surfactant proteins A and D from the lung lavage of alveolar proteinosis patients and from pooled amniotic fluid. *J Immunol Methods.* 1998 Nov 1;220(1-2):139-49
- Teclé T, White MR, Crouch EC, Hartshorn KL.. Inhibition of influenza viral neuraminidase activity by collectins. *Arch Virol.* 2007;152(9):1731-42. Epub 2007 May 22.
- Theoharides TC, Boucher W, Spear K. Serum interleukin-6 reflects disease severity and osteoporosis in mastocytosis patients. *Int Arch Allergy Immunol.* 2002 Aug;128(4):344-50.
- Van de Wetering JK, van Golde LM, Batenburg JJ. Collectins: players of the innate immune system. *Eur J Biochem.* 2004 Apr;271(7):1229-49.
- Van Iwaarden JF, van Strijp JA, Ebskamp MJ, Welmers AC, Verhoef J, van Golde LM. Surfactant protein A is opsonin in phagocytosis of herpes simplex virus type 1 by rat alveolar macrophages. *Am J Physiol.* 1991 Aug;261(2 Pt 1):L204-9.
- Weaver TE, Whitsett JA. Function and regulation of expression of pulmonary surfactant-associated proteins. *Biochem J.* 1991 Jan 15;273(Pt 2):249-64.
- Zúñiga J, Torres M, Romo J, Torres D, Jiménez L, Ramírez G, Cruz A, Espinosa E, Herrera T, Buendía I, Ramírez-Venegas A, González Y, Bobadilla K, Hernández F, García J, Quiñones-Falconi F, Sada E, Manjarrez ME, Cabello C, Kawa S, Zlotnik A, Pardo A, Selman M. Inflammatory profiles in severe pneumonia associated with the pandemic influenza A/H1N1 virus isolated in Mexico City. Autoimmunity. 2011 Nov;44(7):562-70. doi: 10.3109/08916934.2011.592885.

Table 1: Target Genes, Forward and Reverse primers used for qPCR

Target	Forward Primer	Reverse Primer
18S	5'-ATGGCCGTTCTTAGTTGGTG-3'	5'-CGCTGAGCCAGTCAGTGTAG-3'
IL-6	5'-GAAAGCAGCAAAGAGGCACT-3'	5'-TTTCACCAGGCAAGTCTCCT-3'
IL-12	5'-AACTTGCAGCTGAAGCCATT-3'	5'-GACCTGAACGCAGAATGTCA-3'
TNF-α	5'-AGCCCATGTTGTAGCAAACC-3'	5'-TGAGGTACAGGCCCTCTGAT-3'
M1	5'AAACATATGTCTGATAACGAAGGAGA ACAGTTCTT-3'	5'GCTGAATTCTACCTCATGGTCTTC TTGA-3'
RANTES	5'-GCGGGTACCATGAAGATCTCTG-3'	5'-GGGTCAGAATCAAGAAACCCTC- 3'
IFN-α	5'-TTT CTC CTG CCT GAA GGA CAG-3'	5'-GCT CAT GAT TTC TGC TCT GAC A-3'

Figure Legends

Figure 1: SDS-PAGE (15% w/v) analysis of expression and purification of a recombinant fragment of Human Surfactant protein (rfhSP-A). pUK-A1 construct containing neck and CRD region was expressed under T7 bacteriophage in *Escherichia coli* BL21 (λ DE3) pLysS. Following IPTG induction, the expressed bacterial cells show rfhSP-A overexpression at ~18 kDa. The inclusion bodies were refolded and affinity purified using a mannose-agarose column.

Figure 2: Binding of rfhSP-A to (A) pH1N1 and (B) H3N2 via ELISA. Microtiter wells were coated with varied concentrations of FLSP-A, rfhSP-A and rfhSP-D (10, 5, 2.5, and 1.25 μ g/ml). 20 μ l of concentrated pH1N1 or H3N2 virus (1.36×10^6 pfu/ml) was diluted in 200 μ l of PBS + 5 mM CaCl₂ and 10 μ l of the diluted virus was added to all the wells, and probed with either monoclonal anti-influenza virus H1 or polyclonal anti-influenza virus H3 antibody. VSV-G pseudotyped lentivirus was used as a negative RNA virus control. The data were expressed as mean of three independent experiments done in triplicates \pm SEM

Figure 3: Cell-binding assay to show binding of (A) pH1N1 and (B) H3N2 pre-incubated with rfhSP-A to A549 cells. Microtiter wells were coated with A549 cells (1×10^5 cells/ml) and incubated overnight at 37°C. Different concentrations of rfhSP-A (10, 5, 2.5, and 1.25 μ g/ml) pre-incubated with pH1N1 and H3N2 virus were added to the corresponding wells, followed by incubation at room temperature for 2 h. After fixing the cells with 4% paraformaldehyde, monoclonal anti-influenza virus H1, or polyclonal anti-influenza virus H3 antibodies were added to the corresponding wells. Maltose-binding protein (MBP) was used as a negative control protein. The data were expressed as mean of three independent experiments carried out in triplicates \pm SEM

Figure 4: (A) Far western blot analysis to show rfhSP-A binding to purified pH1N1 and H3N2. 10 µl of concentrated virus (1.36×10^6 pfu/ml) was first run on the SDS-PAGE under reducing conditions, and then transferred onto a nitrocellulose membrane and incubated with 10µg of rfhSP-A. The membrane was probed with anti-rabbit SP-A polyclonal antibody. rfhSP-A bound to NA (~60 kDa), M1 (~25 kDa) and M2 (~17kDa) in the case of both pH1N1 and H3N2 subtypes. The identity of SP-A bound IAV proteins was validated using a separate blot that was directly probed with monoclonal anti-NA, M1 and M2 antibodies (B). **(C) Direct ELISA to show the ability of rfhSP-A to bind purified recombinant neuraminidase (NA) of IAV.** VSV-G was used as a negative control protein, where no significance binding was detected. The data were expressed as mean of three independent experiments carried out in triplicates \pm SEM. Significance was determined using the unpaired one-way ANOVA test (**p< 0.0001)(n= 3

Figure 5: rfhSP-A treatment promotes infection and replication (A), while suppression of M1 replication was seen with FLSP-A (B) of pH1N1 and (B) H3N2 in target human A549 cells. M1 expression of both pH1N1 and H3N2 influenza A virus (IAV) (MOI 1) after infection of A549 cells at 2 and 6 h. A549 cells were incubated with pH1N1 and H3N2 pre-incubated with or without purified rfhSP-A and FLSP-A (10 µg/ml). Cell pellets were harvested at 2 and 6 h to analyze the M1 expression of IAV. Cells were lysed, and purified RNA extracted was converted into cDNA. Infection was measured via qRT-PCR using M1 primers; 18S was used as an endogenous control. Results shown are normalized to M1 levels at 2 h untreated. Significance was determined using the unpaired one-way ANOVA test (**p< 0.01, ***p< 0.001, and ****p< 0.0001) (n= 3). UT (un-treated sample), and T (treated sample).

Figure 6: Differential mRNA expression profile of selected cytokines/chemokines produced by A549 cells challenged with pH1N1 and H3N2 pre-incubated with rfhSP-A (A&B) and FLSP-A (C&D). The expression levels of selected cytokines and chemokine were

measured using qRT-PCR and the data were normalized via 18S rRNA expression as a control. The relative expression (RQ) was calculated by using cells only time point as the calibrator. The RQ value was calculated using the formula: $RQ = 2^{-\Delta\Delta Ct}$. Assays were conducted in triplicates and error bars represent \pm SEM. Significance was determined using the unpaired one-way ANOVA test (** $p < 0.01$, *** $p < 0.001$, and **** $p < 0.0001$) (n=3). UT (untreated sample), and T (treated sample).

Figure 7: mRNA expression levels of pro-inflammatory cytokine, interferon (IFN) α in untreated and rfhSP-A (A) and FLSP-A (B) treated pH1N1 and H3N2 subtype of IAV.

The expression levels of cytokines and chemokine were measured using qRT-PCR and the data were normalized via 18S rRNA expression as an endogenous control. The relative expression (RQ) was calculated by using cells only time point as the calibrator. The RQ value was calculated using the formula: $RQ = 2^{-\Delta\Delta Ct}$. Assays were conducted in triplicates and error bars represents \pm SEM. Significance was determined using the unpaired one-way ANOVA test (* $p < 0.05$, ** $p < 0.01$, *** $p < 0.001$, and **** $p < 0.0001$) (n= 3 UT (untreated sample), and T (treated sample)).

Figure 8: Multiplex cytokine array analysis of supernatants collected at 24 h time point.

A549 cells were challenged with (A) pH1N1 and (B) H3N2, following rfhSP-A (10 μ g/ml) treatment. TNF- α , IL-6, IL-8, IL-12p40 and MCP-1 were measured using a commercially available MagPix Milliplex kit (EMD Millipore). Experiment was conducted in duplicates and error bars represent \pm SEM (n= 3); significance was determined using unpaired one-way ANOVA test (* $p < 0.05$, ** $p < 0.01$, *** $p < 0.001$ and **** $p < 0.0001$). UT (untreated sample), and T (treated sample).

Figures

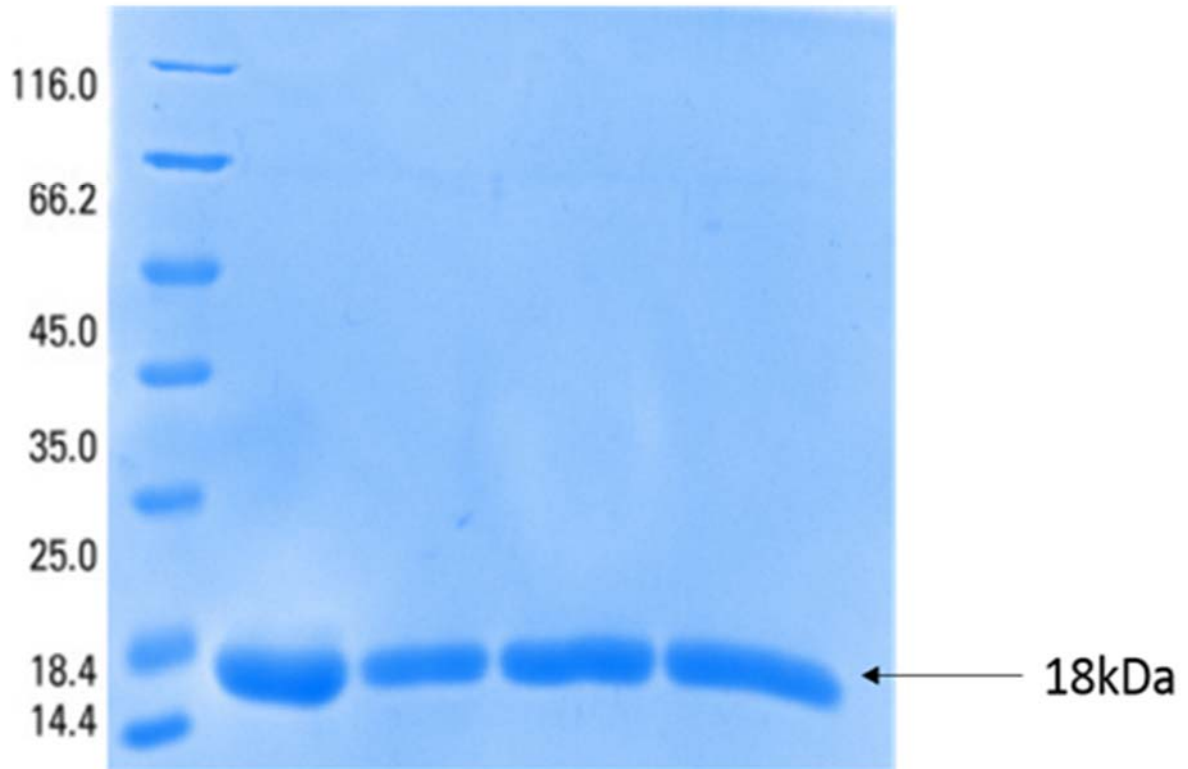
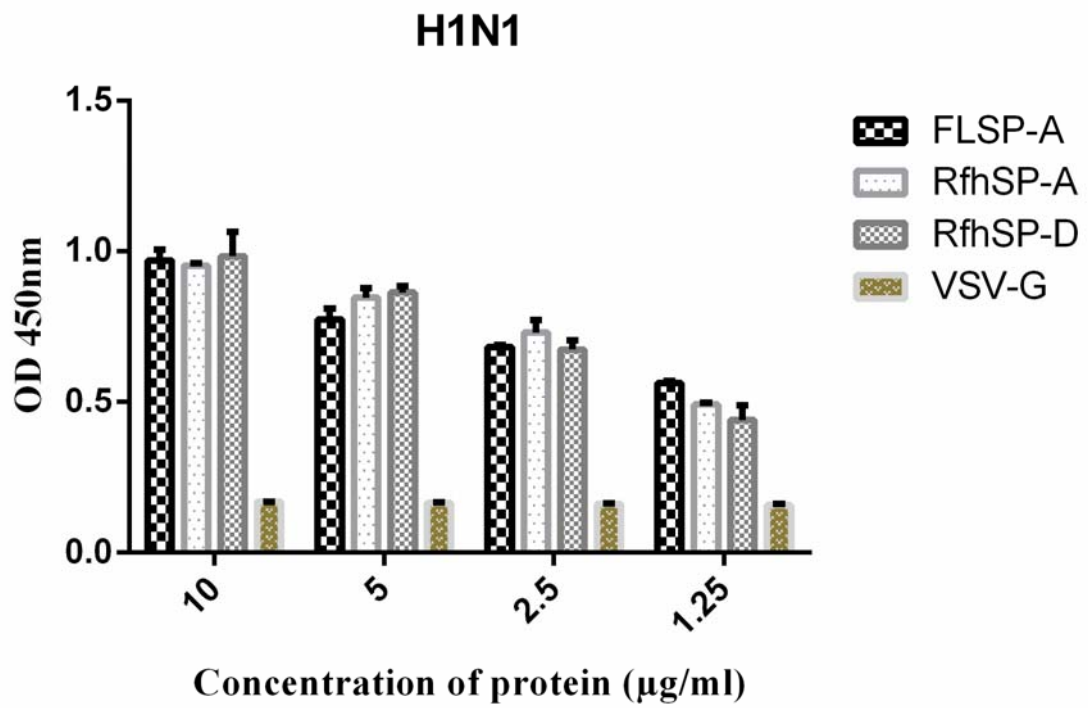


Figure 1

A



B

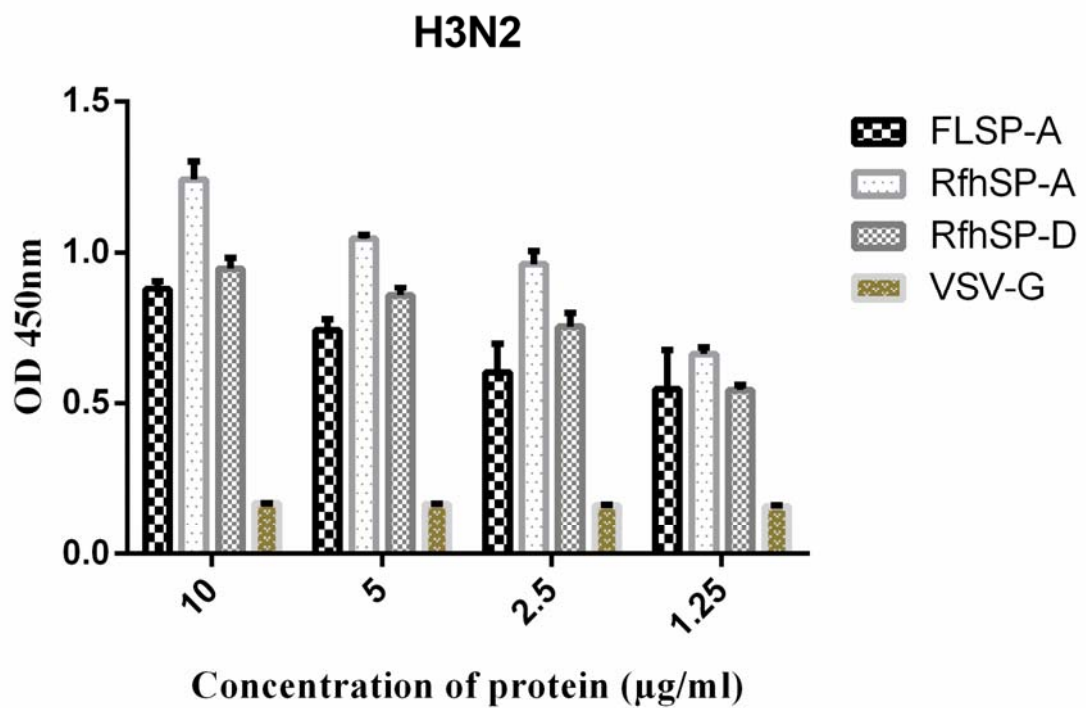
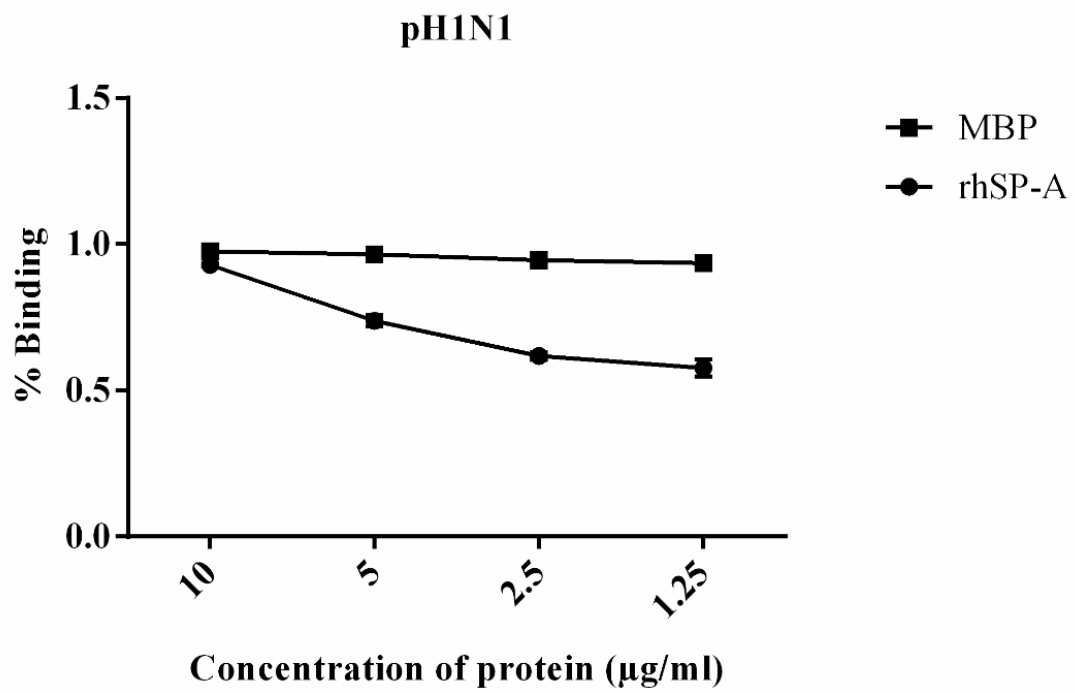


Figure 2

A



B

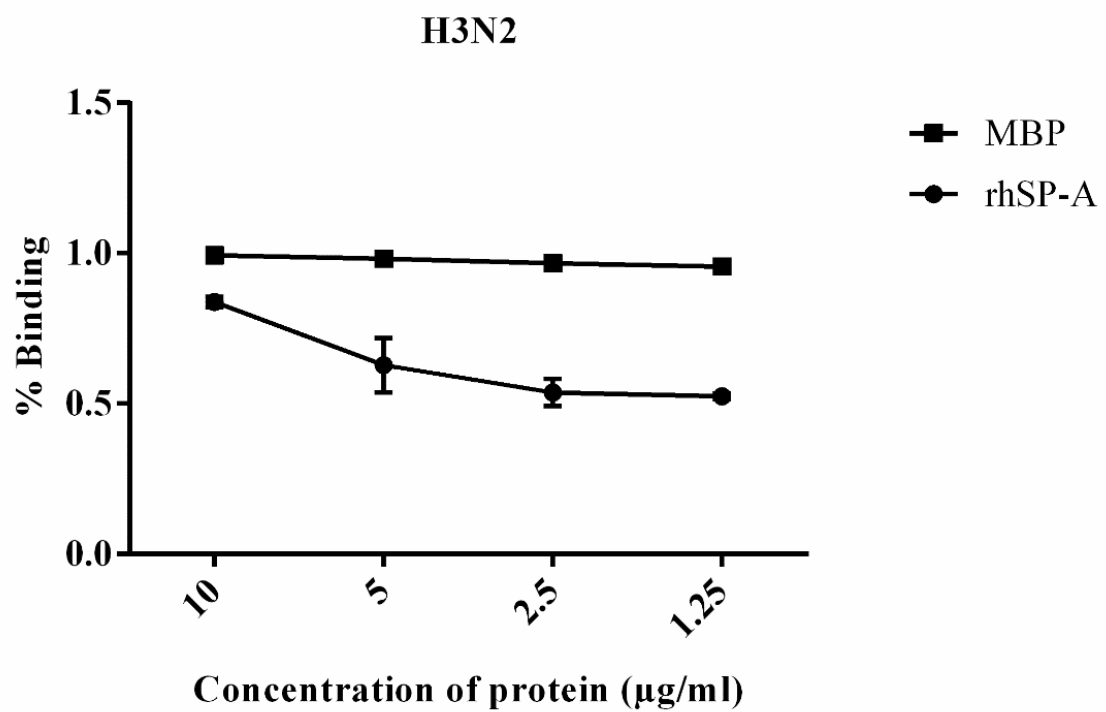


Figure 3

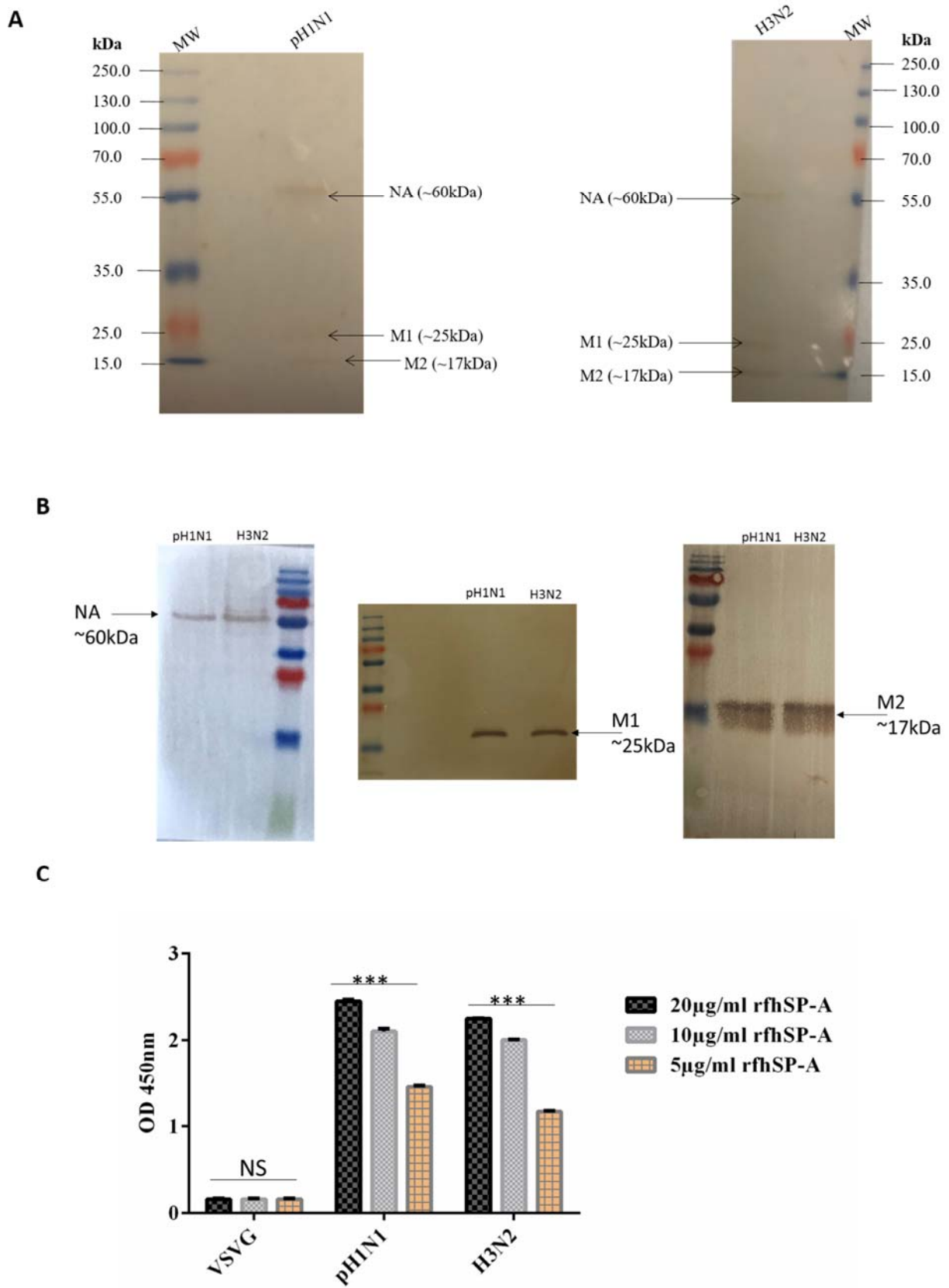
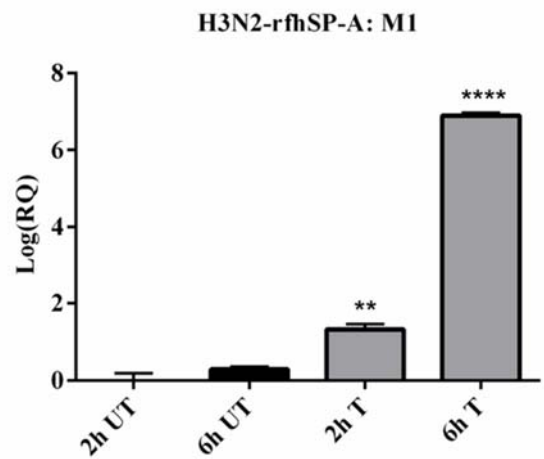
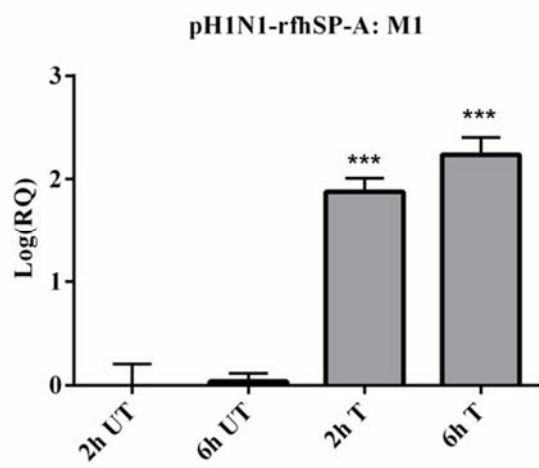


Figure 4

A



B

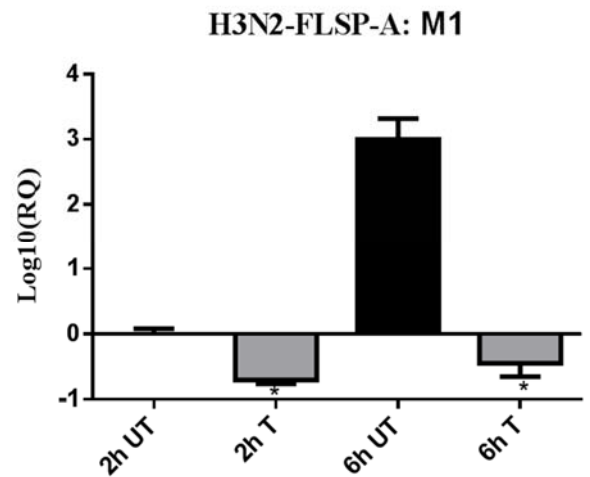
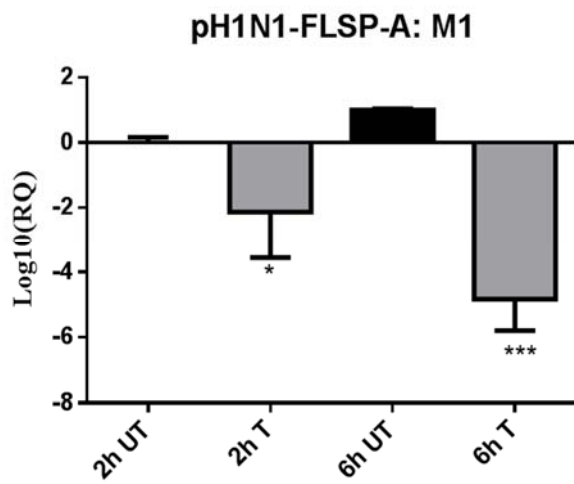


Figure 5

A

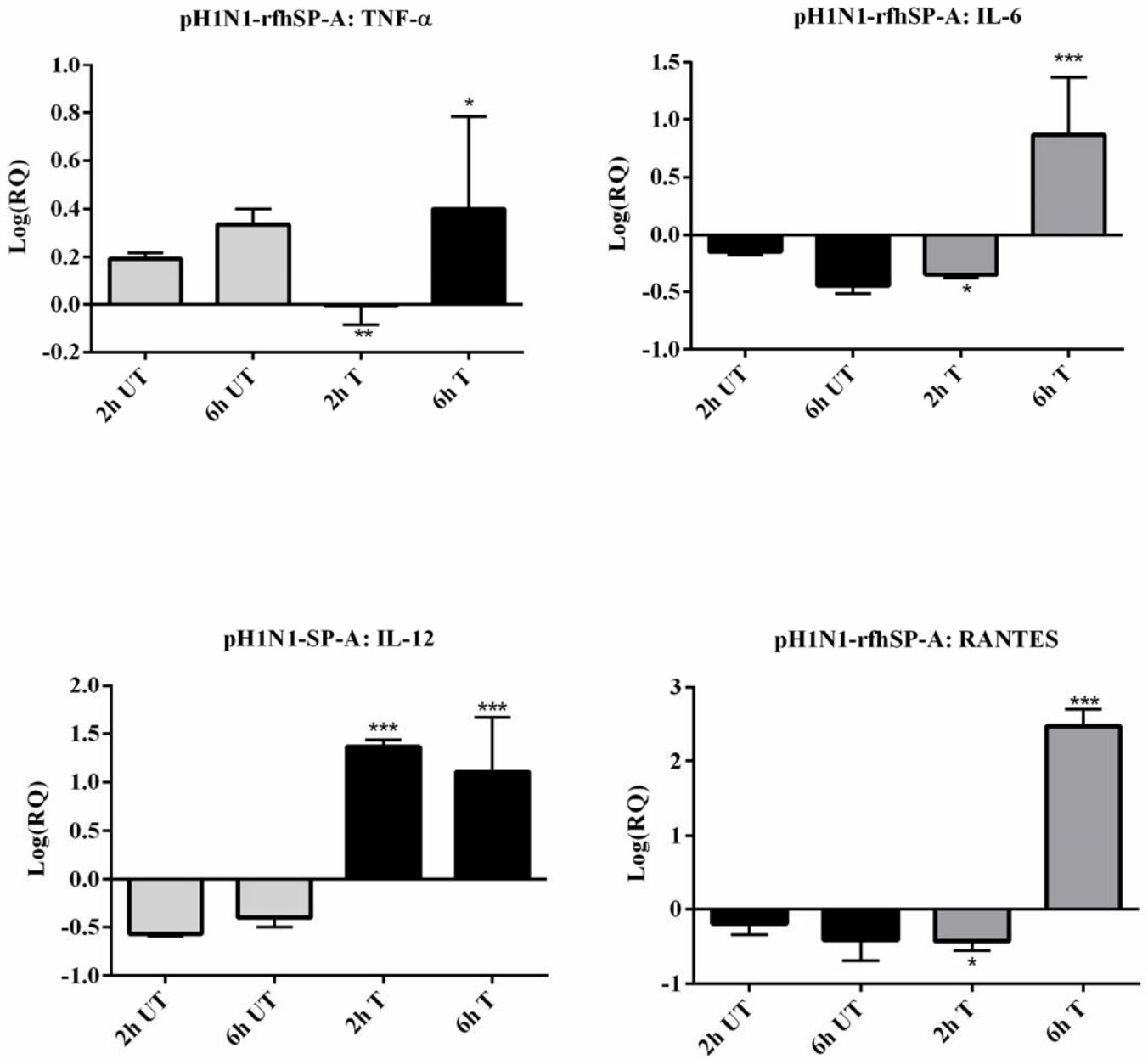


Figure 6A

B

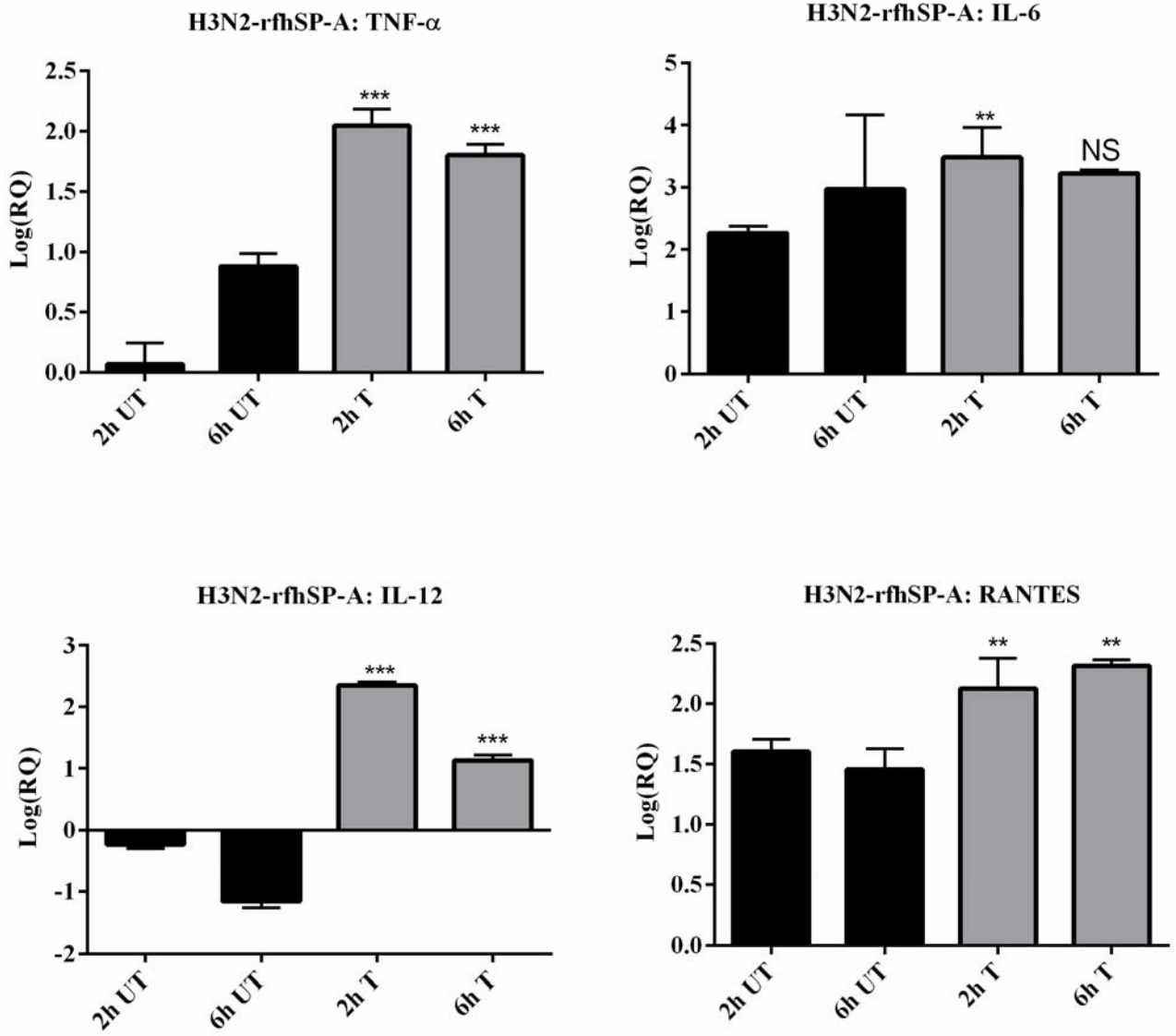


Figure 6B

C

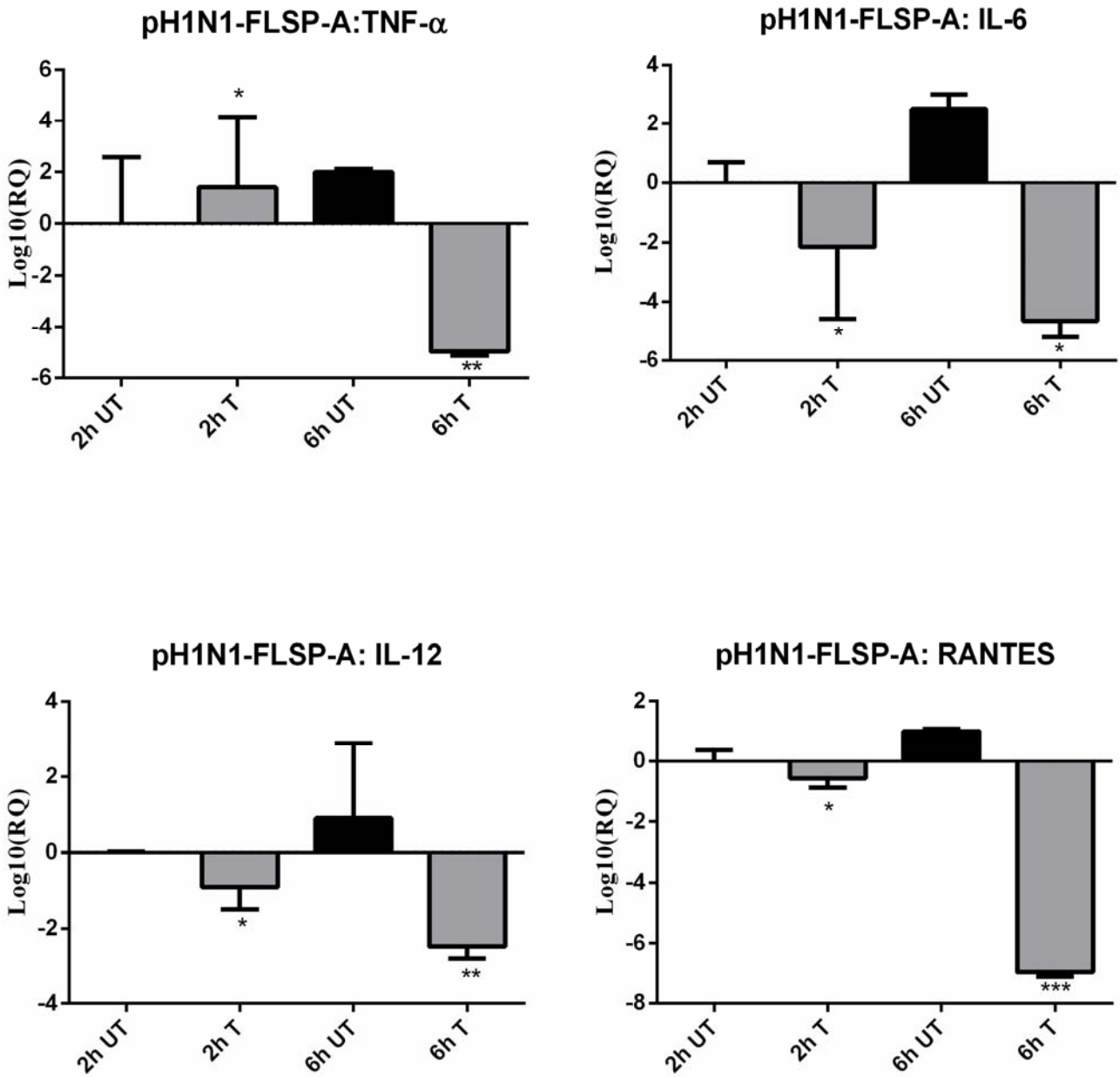


Figure 6C

D

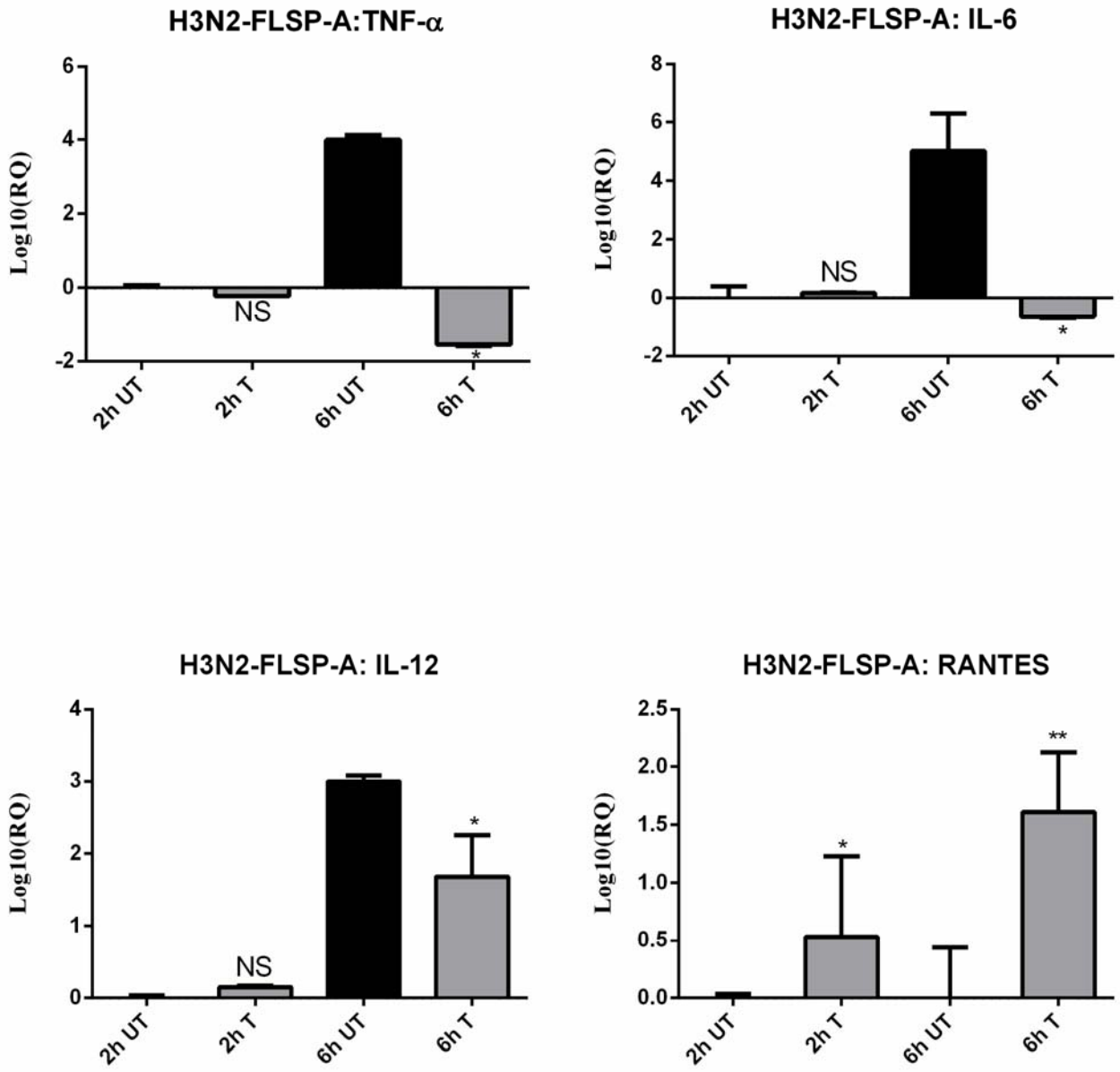
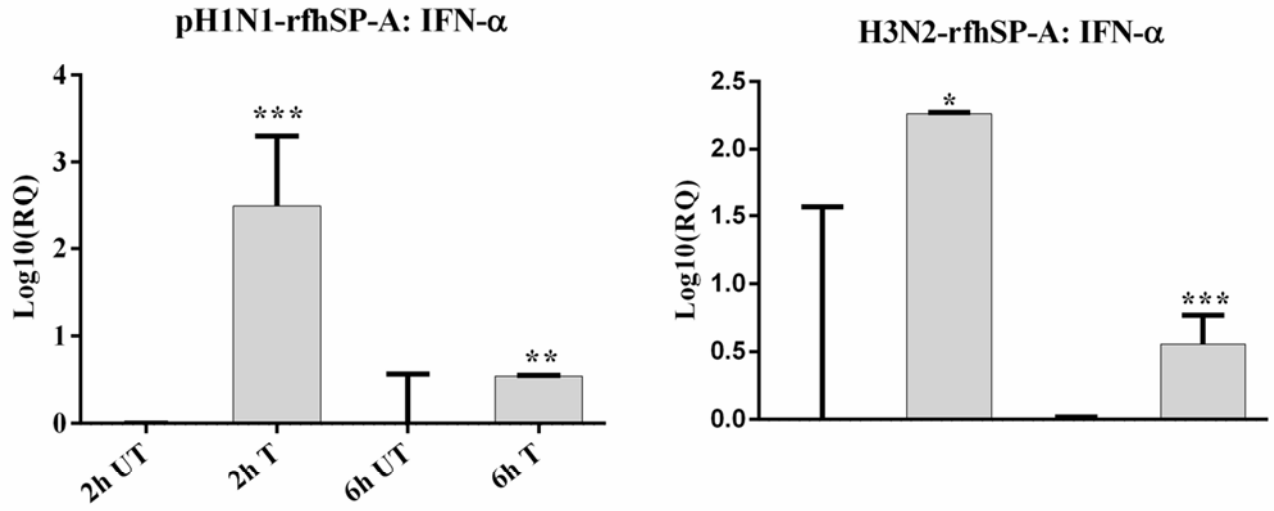


Figure 6D

A



B

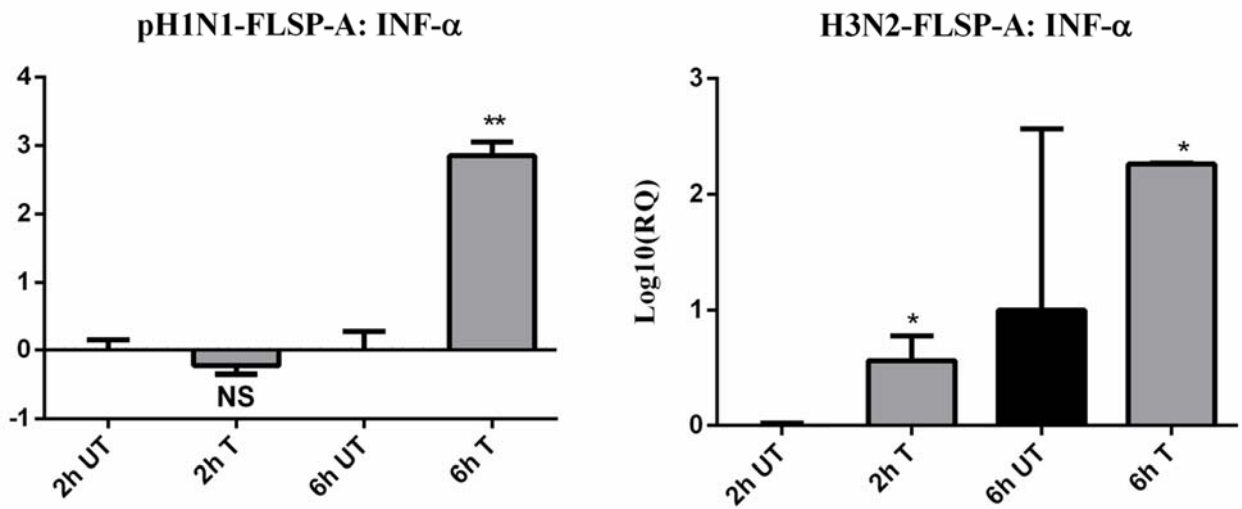


Figure 7

A

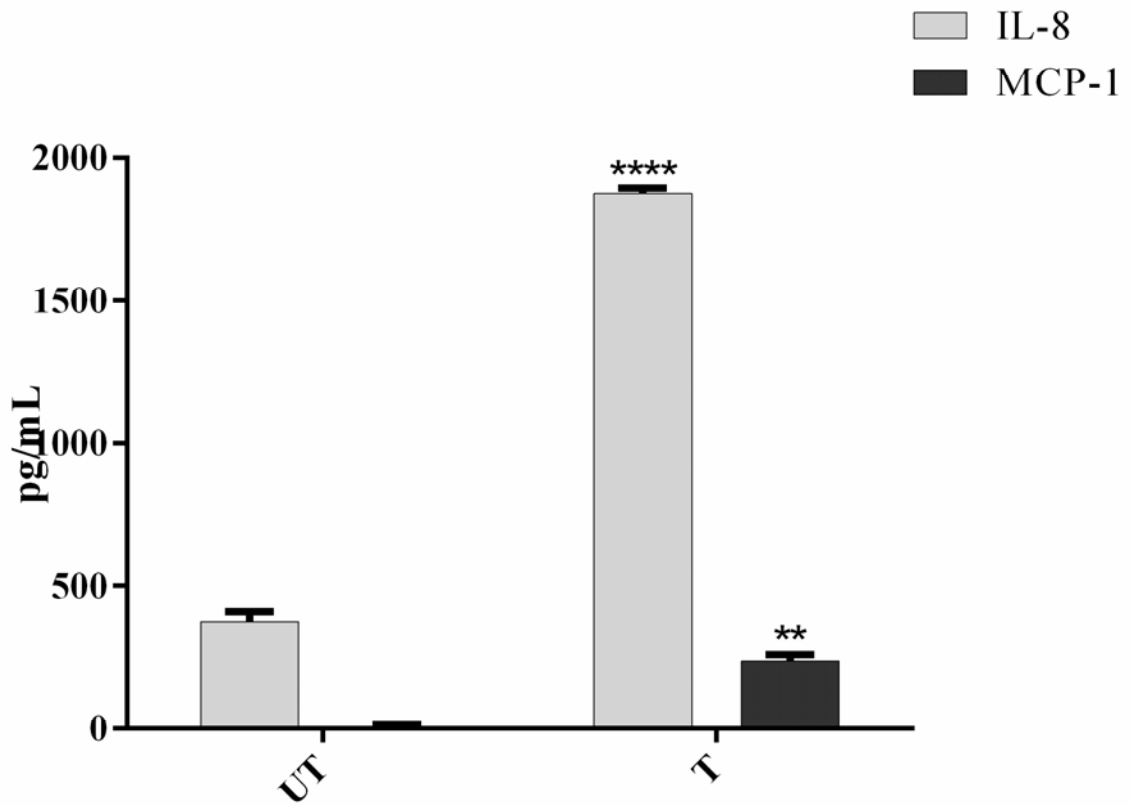
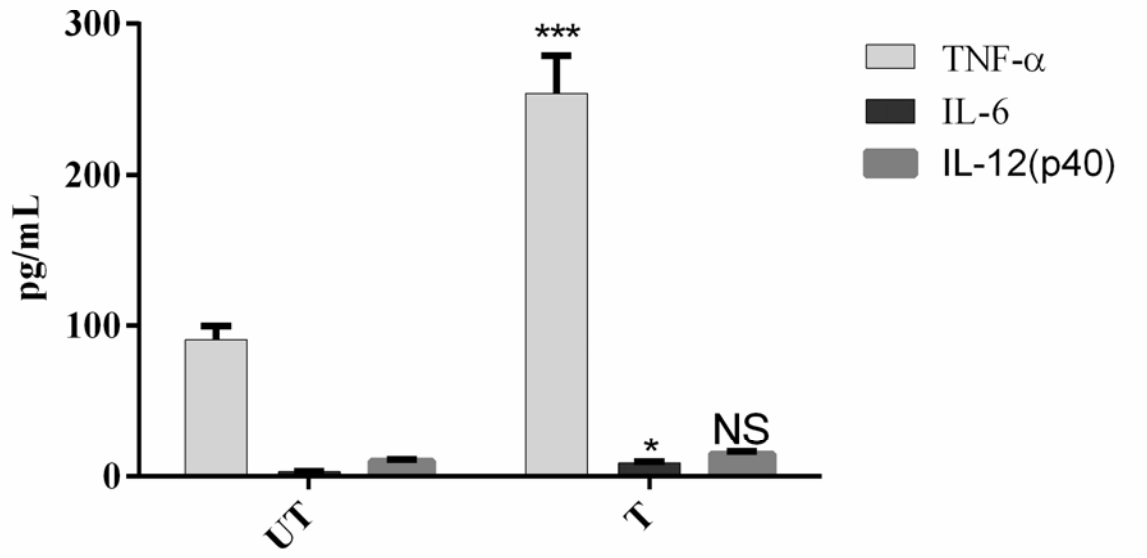


Figure 8A

B

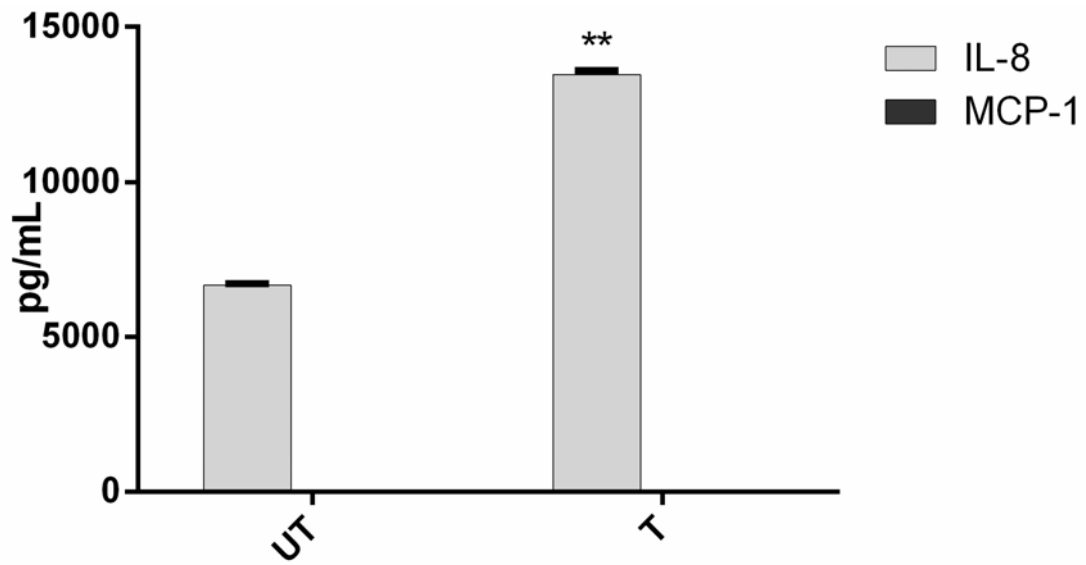
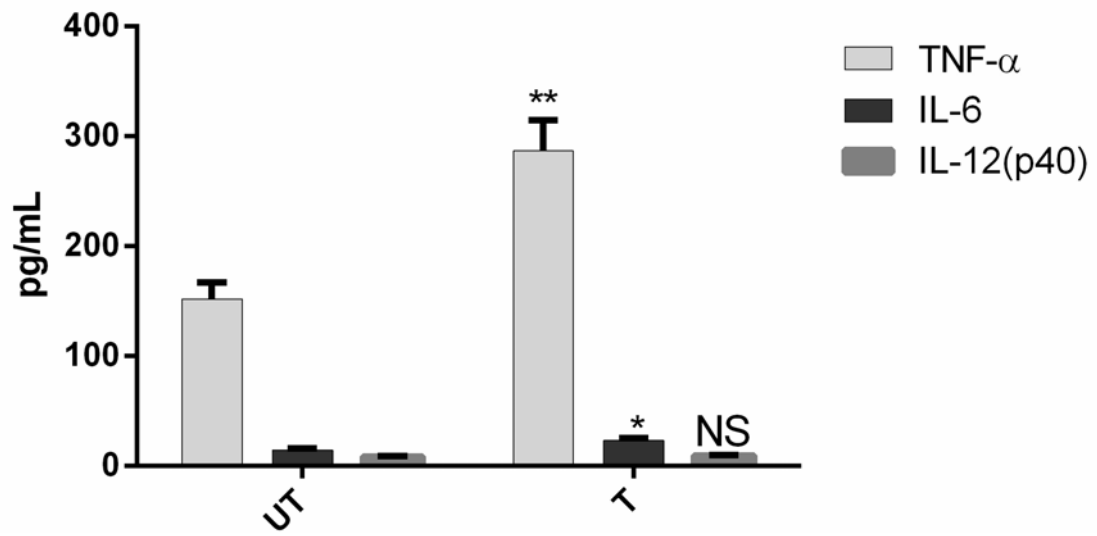


Figure 8B